ACS Catalysis

pubs.acs.org/acscatalysis Letter

Pyridylmethyl Radicals for Enantioselective Alkene Hydroalkylation Using "Ene"-Reductases

Sophie G. Bender and Todd K. Hyster*

Cite This: *ACS Catal.* 2023, 13, 14680−14684 Read Online

ACCESS | Metrics & More | Article Recommendations | Supporting Information

ABSTRACT: Aromatic electron-deficient heterocycles, such as pyridines, are found in many biologically relevant structures, including those with medicinal applications. Methods for their substitution can streamline the synthesis of valuable molecules and allow access to unexplored chemical space. However, enantioselective methods for these derivatizations remain lacking, especially at remote stereocenters. Here, we present a photoenzymatic reaction for the reductive coupling of electron-deficient heterocycles with alkenes using flavin-dependent "ene"-reductases. This transformation results in the generation of a γ-stereocenter with high enantioselectivity. We propose that this light-driven transformation proceeds via excitation of a transient enzyme−substrate complex, enabling the enzyme to access the reductive potential needed for radical initiation when the substrates are bound in the active site. This work represents a stereoselective method for synthesizing derivatives of pyridine and similar heterocycles and an expansion of the substrate capabilities of "ene"-reductases in chemical synthesis.

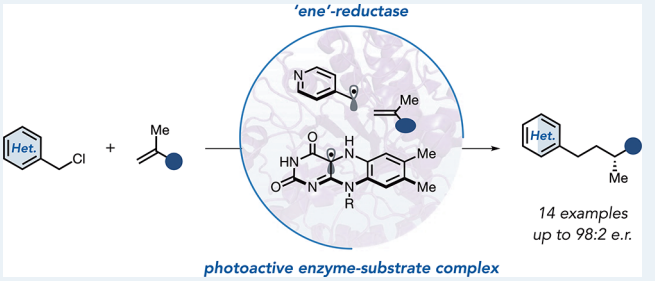

KEYWORDS: *biocatalysis, pyridines, photochemistry, asymmetric synthesis, radical chemistry*

Pyridine-based scaffolds are indispensable among pharmaceutically relevant small molecules, and methods for their derivatization are mainstays in the medicinal synthetic toolkit.[1,2] Many strategies toward the synthesis of substituted pyridines have been developed, employing both ring-building and derivatization approaches.[3−5] However, many of these methods cannot introduce stereochemical information, as is the case with most azine C−H functionalization[6,7] and cross-coupling strategies.[8] Pyridines' ligand functionality has long stymied the development of metal-catalyzed methods,[9] and when asymmetric methods are successful, control over the new stereocenter is usually confined to proximal α- or β-positions.[10−15] Strategies to access γ-stereoenriched pyridines are substantially more rare, relying on the asymmetric addition of prochiral radicals into vinylpyridines.[16−18] As drug discovery ventures into three-dimensional space, more diverse methods will be required to access these sp^3-rich molecules with high selectivity rapidly.[19] Our group envisioned that a biocatalytic method could impart control over constructing a remote pyridyl γ-stereocenter from readily available α-halopyridines, efficiently increasing the complexity of simple heterocyclic structures.

Previous work in our lab and others has demonstrated that flavin-dependent "ene"-reductases (EREDs) can catalyze various stereoselective C−C,[20−26] C−N,[27,28] C−O,[29] and C−S[30] bond forming reactions. Due to their favorable redox properties as well as similarity to other ERED substrates,[31] methods for C_{sp3}−C_{sp3} bond formation have frequently utilized α-halocarbonyl compounds as radical precursors. For easily reduced substrates, such as α-bromo ketones, electron transfer from the fully reduced flavin cofactor (FMN_{hq}) occurs in the ground state.[25] When using less reactive substrates, such as α-chloroamides or alkyl iodides, electron transfer can be initiated by exciting enzyme-templated charge-transfer (CT) complexes formed between the substrates and FMN_{hq}.[20−24,26,32,33] Based on these activation modes, we questioned whether alkyl halides lacking the carbonyl binding handle could serve as radical precursors. We decided to apply this approach to constructing pyridine derivatives to develop a highly selective process compatible with these desirable structures (see Figure 1).

We began by examining the coupling of 4-(chloromethyl)-pyridine **1** with α-methylstyrene **2** catalyzed by an ERED from *Gluconobacter oxidans* (GluER-T36A) (Figure 2). This single mutant ERED was selected based on its success catalyzing other reductive coupling reactions in our lab previously.[20,23,24,33,34] Although protonated 4-(chloromethyl)-pyridine **1** is significantly less challenging to reduce ($E_{p/2}$ = −0.72 V vs SCE) than chloroamides ($E_{p/2}$ = −1.65 V vs

Received: August 11, 2023
Revised: October 25, 2023
Accepted: October 27, 2023
Published: October 31, 2023

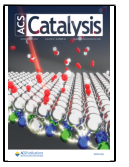

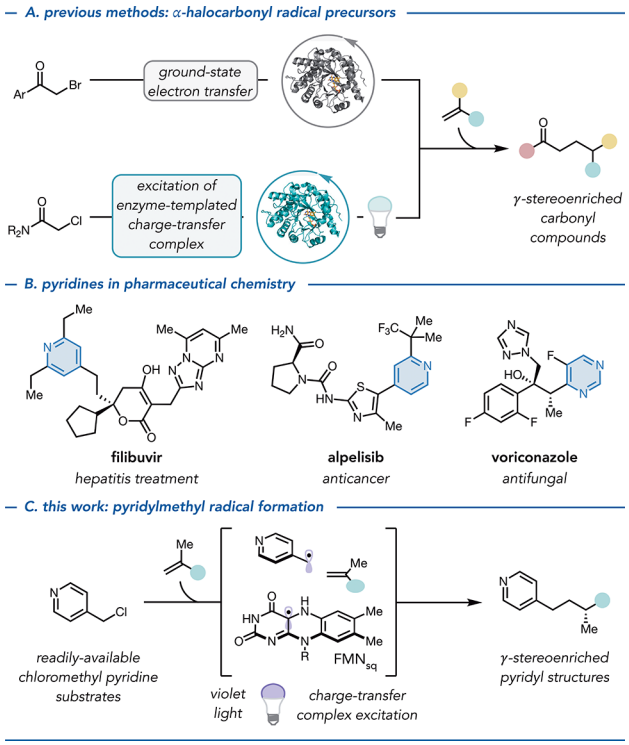

Figure 1. Precedent for and utility of biocatalytic coupling with pyridyl structures. A. Electron transfer initiation strategies in EREDs. B. Selected drug molecules bearing electron-deficient heterocycles. C. Expansion of ERED strategies to pyridyl structures.

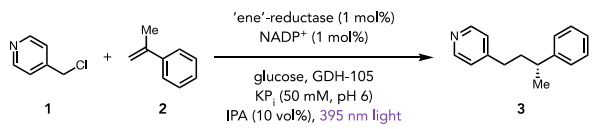

entry[a]	conditions[b]	yield 3[c]	e.r. 3[d]
1	GluER T36A	55%	96:4
2	ERED from *G. morbifer* (MonstER)	68%	94:6
3	ERED from *G. kanchanaburiensis*	48%	90:10
4	ERED from *G. japonicus*	46%	80:20
5	ERED from *G. thailandicus*	45%	88:12
6	ERED from *G. cerinus*	42%	84:16
7	ERED from *G. frateurii*	45%	87:13
8	no enzyme	0%	n.d.
9	FMN instead of ERED[e]	0%	n.d.

Figure 2. GluER homolog screen. [a]Standard conditions: **1** (10.0 μmol, 1.64 mg of hydrochloride salt), NaOH (10 μL of 1 M solution in water), **2** (40.0 μmol), "ene"-reductase (0.1 μmol), $NADP^+$ (0.1 μmol), glucose (21.0 μmol), GDH-105 (20 wt %, 0.3 mg), isopropanol (137.5 μL), buffer (50 mM KP_i pH 6, to a total volume of 1375 μL), 18 h, 25 °C. [b]Purified "ene"-reductase; full sequence information included in the Supporting Information. [c]Assay yield determined by LCMS against a 1,3,5-tribromobenzene internal standard. Standard curve is included in the Supporting Information. [d]Enantiomeric ratio (*R*:*S*) determined by HPLC; n.d. = not determined. [e]Reaction was run with FMN (0.1 μmol) instead of enzyme.

SCE[20]) or chloroketones ($E_{p/2}$ = −1.44 V vs SCE[35]), no product was observed in the absence of light. However, upon irradiation with high-intensity cyan LEDs, coupled product **3** was formed in 36% yield alongside 45% yield of 4-methylpyridine **4**, the product of starting material hydrodehalogenation. Following a screen of multiple different light setups (Table S1), the best results were observed using lower-intensity violet LEDs, which afforded the desired product in 55% yield with only 14% of **4**.

To improve the yield of this transformation, we prepared a collection of GluER homologs from other species in the *Gluconobacter* genus and tested them as catalysts. One "ene"-reductase from each of the 6 species was chosen based on sequence similarity and expressed; of these, a wild-type oxidoreductase from *Gluconobacter morbifer* dubbed MonstER was discovered to effect the model reaction in 68% yield and 94:6 e.r. (Figure 2).

Intrigued by the apparent dependence of yield and product distribution on irradiation wavelength, we performed a systematic study of different wavelengths with control over the irradiation intensity. By standardizing the reaction setups and photon flux, an approximation of an action spectrum could be obtained, providing a profile of the activity of this system under different energies of light (Figures 3 and S7, Tables S5–

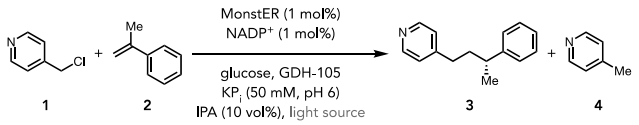

entry[a]	light[b]	1 remaining[c]	yield 3[c]	e.r. 3[d]	yield 4[c]	ratio 3:4
1	near-UV (365 nm)	21%	21%	83:17	7%	3.3
2	violet (395 nm)	0%	71%	94:6	23%	3.0
3	indigo (445 nm)	5%	56%	93:7	40%	1.4
4	blue (470 nm)	56%	17%	94:6	27%	0.65
5	cyan (505 nm)	88%	1%	n.d.	7%	0.09
6	red (630 nm)	95%	0%	n.d.	2%	—
7	no light	96%	0%	n.d.	0%	—

Figure 3. Wavelength studies. [a]Standard conditions: **1** (10.0 μmol, 1.64 mg of hydrochloride salt), NaOH (10 μL of 1 M solution in water), **2** (40.0 μmol), MonstER (0.1 μmol), $NADP^+$ (0.1 μmol), glucose (21.0 μmol), GDH-105 (20 wt %, 0.3 mg), isopropanol (137.5 μL), buffer (50 mM KP_i pH 6, to a total volume of 1375 μL), 18 h, 25 °C. [b]Irradiation was conducted using standardized setups with similar intensity (see the Supporting Information). [c]Assay yield was determined by HPLC against 1,3,5-tribromobenzene internal standard. Standard curve included in the Supporting Information. [d]Enantiomeric ratio (*R*:*S*) determined by HPLC; n.d. = not determined.

S7). This would allow us to begin to characterize the various photoactive species present in the reaction mixture, the excitation of which could be leading to different mechanistic pathways.

The desired product **3** is formed across a broad range of wavelengths from near-UV (365 nm) to cyan (505 nm), with maximum formation using violet (395 nm) and indigo (445 nm). As the published emission of these LEDs spectra have minimal overlap with the absorption of FMN_{hq}, direct excitation of the cofactor alone may not be sufficient to explain this reactivity.[36] The light source displaying the closest overlap with FMN_{hq} is the 365 nm LED (Figures S5, S8, and S9); however, this gave poor overall yields. This is likely due to a combination of enzyme and substrate decomposition under high-energy irradiation. Formation of the hydrodehalogenated byproduct **4** showed a different trend, with maximal formation under indigo (445 nm) irradiation, and small amounts could be observed under all light sources used, including red (630 nm). This different wavelength dependence results in a product ratio that changes across the wavelengths studied, with a distribution biased toward **3** at short wavelengths and **4** at long wavelengths.

https://doi.org/10.1021/acscatal.3c03771
ACS Catal. 2023, 13, 14680−14684

Based on these results, we propose that there are two important photoactive enzyme-substrate complexes generated in this reaction. One of these complexes has an absorbance maximum between 365 and 445 nm and favors the formation of the desired product **3**. This complex likely contains **1** and **2** oriented optimally for carbon−carbon bond formation upon α-pyridyl radical initiation, resembling the quaternary charge-transfer complex previously observed between α-chloroamides and α-methylstyrene in GluER T36A.[23] The second complex has an absorbance maximum between 445 and 470 nm, and excitation of this complex leads preferentially to formation of hydrodehalogenated byproduct **4**. We hypothesize that this complex lacks the alkene, consequently resulting in only hydrodehalogenation. Indeed, control experiments with 1 equiv of α-methylstyrene **2** result in a 1.5:1 ratio of coupled product **3** to the hydrodehalogenated product **4** (Table S4). This result suggests that excess alkene is required to favor formation of the CT complex composed of the alkene, chloromethylpyridine, FMN_{hq}, and the protein. Unfortunately, these complexes are difficult to observe via UV−visible spectroscopy, potentially because of the poor substrate solubility under the conditions suitable for spectroscopic measurements (Figure S5). We believe that these wavelength studies provide substantial evidence for their existence.

Having selected violet LEDs (395 nm) as the best irradiation source for coupled product formation, MonstER was used to explore the scope of this transformation (Figure 4). A methyl substituent on the pyridyl ring is well-tolerated (**18**), and interestingly, the 2,6-dimethyl substituted material gave a product (**19**) comparable in yield (61%) to the unsubstituted model system with somewhat lower enantioselectivity. Given that these methyl substituents create substantial steric bulk around the pyridyl nitrogen, this suggests that effective hydrogen bonding to this nitrogen is not required for productive substrate binding. However, it may play a role in the geometry of the enantiodetermining step. A pyridine ring bearing a 3-bromo substituent was also competent in the reaction (**20**), providing a potential handle for further derivatization. The 2-(chloromethyl)pyridine substrate **8** gave a product (**21**) in lower yield but still very high enantioselectivity. We screened a diverse collection of EREDs on substrate **8** (Table S2), and though none of them had a higher yield than MonstER, the enzyme OYE1 stood out for having reversed the enantiomeric preference of the product (4:96 e.r.).

A variety of quinolyl and isoquinolyl compounds (**22**−**25**) were also competent substrates. Notable among this category is the very wide range in selectivities, from the almost racemic 4-quinolyl to the highly selective 1-isoquinolyl. Again, we suspect that these results provide a window into the role of substrate binding geometry in the selectivity of the terminating hydrogen atom transfer step. A pyrimidyl starting material was also tested, giving product (**26**) in moderate yield with excellent enantioselectivity. On the alkene side, a *p*-methoxy styrene partner maintained comparable yields (**27**) to the model system with some stereoselectivity. Vinylpyridines in 2- and 4-substitution patterns (**28** and **29**) were also effective coupling partners, affording dipyridyl structures in moderate yields but with limited enantioselectivity. Lastly, an allyl alcohol partner is also accepted in a moderate yield (**30**) with some selectivity. This structural departure demonstrates that this reaction is not limited to vinyl arene substrates but might instead accommodate a variety of nonstyrenyl coupling partners.

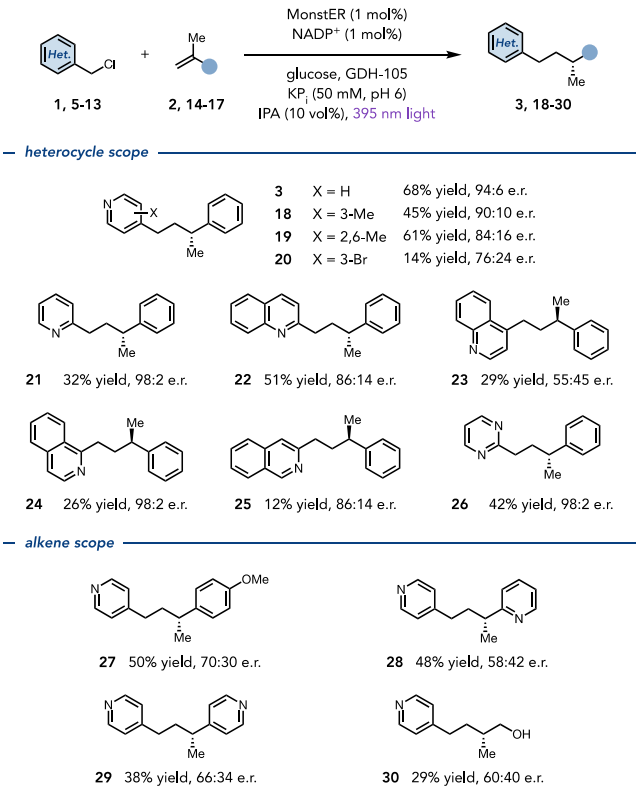

Figure 4. Reaction scope investigation. Absolute (*R*)-stereoconfiguration of **3** assigned via HPLC by comparison to authentic (*R*)-**3**; others are tentatively assigned the (*R*)-configuration by analogy. Standard conditions: (chloromethyl)heteroarene (10.0 μmol of hydrochloride salt), NaOH (10 μL of 1 M solution in water), alkene (40.0 μmol), MonstER (0.1 μmol), $NADP^+$ (0.1 μmol), glucose (21.0 μmol), GDH-105 (20 wt %, 0.3 mg), isopropanol (137.5 μL), buffer (50 mM KP_i pH 6, to a total volume of 1375 μL), 18 h, 25 °C. Yields determined by ^{1}H NMR against 1,3,5-trimethoxybenzene internal standard. Enantiomeric ratios (major:minor) were determined by HPLC.

Isotopic labeling experiments (Figure 5) were performed to probe the source of the radical-terminating hydrogen atom in MonstER (Table S4 and Figures S2−S4). When reactions are run with D-glucose-1-H_1 in a buffer containing > 95% D_2O (to deuterate active-site residues via solvent exchange that may be

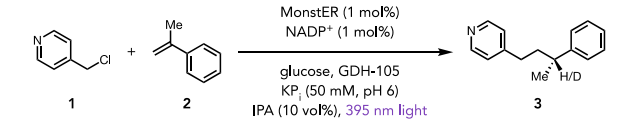

entry[a]	deuterium source[b]	yield 3[c]	e.r. 3[d]	% D-incorporation[e]
1	FMN	41%	89:11	73%
2	buffer	50%	93:7	<5%

Figure 5. Isotopic labeling studies. [a]Standard conditions: **1** (10.0 μmol, 1.64 mg of hydrochloride salt), NaOH (10 μL of 1 M solution in water), **2** (40.0 μmol), GluER T36A (0.1 μmol), $NADP^+$ (0.1 μmol), glucose (21.0 μmol), GDH-105 (20 wt %, 0.3 mg), isopropanol (137.5 μL), buffer (50 mM KP_i pH 6, to a total volume of 1375 μL), 18 h, 25 °C. [b]Deuterated FMN_{hq} was generated *in situ* using D-glucose-1-d_1; deuterated buffer (>95% D_2O) was prepared using D_2O in place of water. [c]Assay yield determined by ^{1}H NMR against a 1,3,5-trimethoxybenzene internal standard. [d]Enantiomeric ratio (*R*:*S*) was determined by HPLC. [e]Deuterium incorporation was determined by ^{13}C NMR.

https://doi.org/10.1021/acscatal.3c03771
ACS Catal. 2023, 13, 14680−14684

potential hydrogen atom sources), < 5% deuterium incorporation is observed, while reactions run with D-glucose-1-d_1 in H_2O buffer (to deuterate flavin at the N5-position via hydride transfer from deuterated NADPH) result in 73% deuterium incorporation at the γ-position. Additionally, using D-glucose-1-d_1 results in somewhat eroded enantioselectivity (89:11 e.r., as opposed to 93:7 e.r. with the D_2O buffer). Taken together, these experiments suggest that hydrogen atom transfer occurs primarily from flavin and that when the flavin is deuterated, the rate of this transfer event is slowed and other hydrogen atom sources in the active site become competitive.

In conclusion, we have developed a biocatalytic method in which halomethylpyridines can be employed as radical precursors for asymmetric hydroalkylations, providing elaborated structures with highly enantioenriched γ-stereocenters. This is enabled through the excitation of substrate-enzyme complexes formed in solution, expanding this technology to noncarbonyl-based substrates that are thus far underutilized in biocatalytic approaches. We anticipate that this strategy will aid in the rapid construction of medicinally relevant scaffolds and set a precedent for this activation mode to be used for a diverse array of nontraditional radical precursors.

■ ASSOCIATED CONTENT

Supporting Information

The Supporting Information is available free of charge at https://pubs.acs.org/doi/10.1021/acscatal.3c03771.

General information; DNA and protein sequence information; experimental procedures; reaction condition optimization; starting materials synthesis and characterization; product characterization; charge transfer complex studies; references; and NMR spectra (PDF)

■ AUTHOR INFORMATION

Corresponding Author

Todd K. Hyster − *Department of Chemistry and Chemical Biology, Cornell University, Ithaca, New York 14850, United States;* Present Address: Department of Chemistry, Princeton University, Princeton, New Jersey 08544, United States; orcid.org/0000-0003-3560-355X; Email: thyster@princeton.edu

Author

Sophie G. Bender − *Department of Chemistry and Chemical Biology, Cornell University, Ithaca, New York 14850, United States;* orcid.org/0000-0003-4578-0832

Complete contact information is available at: https://pubs.acs.org/10.1021/acscatal.3c03771

Notes

The authors declare no competing financial interest.

■ ACKNOWLEDGMENTS

The authors thank Dr. Heather Lam for preliminary studies into the reactivity of 2-(chloromethyl)pyridine, as well as Dr. Felix Raps for help with the synthesis of authentic product standards. We thank Lotus for product purification on select substrates. We also thank Eric Geunes and the Knowles Lab at Princeton University for their help collecting cyclic voltammetry data. The research reported here was supported by the National Science Foundation (CHE-2135973). This work made use of the Cornell University NMR Facility, which is supported, in part, by the NSF through MRI Award CHE-1531632.

■ REFERENCES

(1) De, S.; K, A. K. S.; Kumar Shah, S.; Kazi, S.; Sarkar, N.; Banerjee, S.; Dey, S. Pyridine: The Scaffolds with Significant Clinical Diversity. *RSC Adv.* **2022**, *12* (24), 15385−15406.

(2) Brown, D. G.; Boström, J. Analysis of Past and Present Synthetic Methodologies on Medicinal Chemistry: Where Have All the New Reactions Gone? *J. Med. Chem.* **2016**, *59* (10), 4443−4458.

(3) Hill, M. D. Recent Strategies for the Synthesis of Pyridine Derivatives. *Chemistry − A. European Journal* **2010**, *16* (40), 12052−12062.

(4) Bull, J. A.; Mousseau, J. J.; Pelletier, G.; Charette, A. B. Synthesis of Pyridine and Dihydropyridine Derivatives by Regio- and Stereoselective Addition to N-Activated Pyridines. *Chem. Rev.* **2012**, *112* (5), 2642−2713.

(5) Kumar S, L.; Tabassum, S.; K, S. S.; Govindaraju, S. A Mini Review on the Multicomponent Synthesis of Pyridine Derivatives. *ChemistrySelect* **2022**, *7* (47), No. e202203668.

(6) Murakami, K.; Yamada, S.; Kaneda, T.; Itami, K. C−H Functionalization of Azines. *Chem. Rev.* **2017**, *117* (13), 9302−9332.

(7) Josephitis, C. M.; Nguyen, H. M. H.; McNally, A. Late-Stage C−H Functionalization of Azines. *Chem. Rev.* **2023**, *123*, 7655.

(8) Almond-Thynne, J.; Blakemore, D. C.; Pryde, D. C.; Spivey, A. C. Site-Selective Suzuki−Miyaura Coupling of Heteroaryl Halides − Understanding the Trends for Pharmaceutically Important Classes. *Chem. Sci.* **2017**, *8* (1), 40−62.

(9) Schäfer, P.; Palacin, T.; Sidera, M.; Fletcher, S. P. Asymmetric Suzuki-Miyaura Coupling of Heterocycles via Rhodium-Catalysed Allylic Arylation of Racemates. *Nat. Commun.* **2017**, *8* (1), 15762.

(10) Qiao, B.; Li, C.; Zhao, X.; Yin, Y.; Jiang, Z. Enantioselective Reduction of Azaarene-Based Ketones via Visible Light-Driven Photoredox Asymmetric Catalysis. *Chem. Commun.* **2019**, *55* (52), 7534−7537.

(11) Yin, Y.; Li, Y.; Gonçalves, T. P.; Zhan, Q.; Wang, G.; Zhao, X.; Qiao, B.; Huang, K.-W.; Jiang, Z. All-Carbon Quaternary Stereocenters α to Azaarenes via Radical-Based Asymmetric Olefin Difunctionalization. *J. Am. Chem. Soc.* **2020**, *142* (46), 19451−19456.

(12) Nakano, Y.; Black, M. J.; Meichan, A. J.; Sandoval, B. A.; Chung, M. M.; Biegasiewicz, K. F.; Zhu, T.; Hyster, T. K. Photoenzymatic Hydrogenation of Heteroaromatic Olefins Using 'Ene'-Reductases with Photoredox Catalysts. *Angew. Chem., Int. Ed.* **2020**, *59* (26), 10484−10488.

(13) Trost, B. M.; Thaisrivongs, D. A. Strategy for Employing Unstabilized Nucleophiles in Palladium-Catalyzed Asymmetric Allylic Alkylations. *J. Am. Chem. Soc.* **2008**, *130* (43), 14092−14093.

(14) Trost, B. M.; Thaisrivongs, D. A. Palladium-Catalyzed Regio-, Diastereo-, and Enantioselective Benzylic Allylation of 2-Substituted Pyridines. *J. Am. Chem. Soc.* **2009**, *131* (34), 12056−12057.

(15) Proctor, R. S. J.; Davis, H. J.; Phipps, R. J. Catalytic Enantioselective Minisci-Type Addition to Heteroarenes. *Science* **2018**, *360* (6387), 419−422.

(16) Cao, K.; Tan, S. M.; Lee, R.; Yang, S.; Jia, H.; Zhao, X.; Qiao, B.; Jiang, Z. Catalytic Enantioselective Addition of Prochiral Radicals to Vinylpyridines. *J. Am. Chem. Soc.* **2019**, *141* (13), 5437−5443.

(17) Cao, K.; Li, C.; Tian, D.; Zhao, X.; Yin, Y.; Jiang, Z. Catalytic Enantioselective Reductive Cross Coupling of Electron-Deficient Olefins. *Org. Lett.* **2022**, *24* (26), 4788−4792.

(18) Wang, S.; Li, X.; Liu, H.; Xu, L.; Zhuang, J.; Li, J.; Li, H.; Wang, W. Organocatalytic Enantioselective Direct Additions of Aldehydes to 4-Vinylpyridines and Electron-Deficient Vinylarenes and Their Synthetic Applications. *J. Am. Chem. Soc.* **2015**, *137* (6), 2303−2310.

(19) Lovering, F.; Bikker, J.; Humblet, C. Escape from Flatland: Increasing Saturation as an Approach to Improving Clinical Success. *J. Med. Chem.* **2009**, *52* (21), 6752−6756.

(20) Biegasiewicz, K. F.; Cooper, S. J.; Gao, X.; Oblinsky, D. G.; Kim, J. H.; Garfinkle, S. E.; Joyce, L. A.; Sandoval, B. A.; Scholes, G. D.; Hyster, T. K. Photoexcitation of Flavoenzymes Enables a Stereoselective Radical Cyclization. *Science* **2019**, *364* (6446), 1166−1169.
(21) Fu, H.; Qiao, T.; Carceller, J. M.; MacMillan, S. N.; Hyster, T. K. Asymmetric C-Alkylation of Nitroalkanes via Enzymatic Photoredox Catalysis. *J. Am. Chem. Soc.* **2023**, *145* (2), 787−793.
(22) Gao, X.; Turek-Herman, J. R.; Choi, Y. J.; Cohen, R. D.; Hyster, T. K. Photoenzymatic Synthesis of α-Tertiary Amines by Engineered Flavin-Dependent "Ene"-Reductases. *J. Am. Chem. Soc.* **2021**, *143* (47), 19643−19647.
(23) Page, C. G.; Cooper, S. J.; DeHovitz, J. S.; Oblinsky, D. G.; Biegasiewicz, K. F.; Antropow, A. H.; Armbrust, K. W.; Ellis, J. M.; Hamann, L. G.; Horn, E. J.; Oberg, K. M.; Scholes, G. D.; Hyster, T. K. Quaternary Charge-Transfer Complex Enables Photoenzymatic Intermolecular Hydroalkylation of Olefins. *J. Am. Chem. Soc.* **2021**, *143* (1), 97−102.
(24) Clayman, P. D.; Hyster, T. K. Photoenzymatic Generation of Unstabilized Alkyl Radicals: An Asymmetric Reductive Cyclization. *J. Am. Chem. Soc.* **2020**, *142* (37), 15673−15677.
(25) Fu, H.; Lam, H.; Emmanuel, M. A.; Kim, J. H.; Sandoval, B. A.; Hyster, T. K. Ground-State Electron Transfer as an Initiation Mechanism for Biocatalytic C−C Bond Forming Reactions. *J. Am. Chem. Soc.* **2021**, *143* (25), 9622−9629.
(26) Huang, X.; Wang, B.; Wang, Y.; Jiang, G.; Feng, J.; Zhao, H. Photoenzymatic Enantioselective Intermolecular Radical Hydroalkylation. *Nature* **2020**, *584* (7819), 69−74.
(27) Ye, Y.; Cao, J.; Oblinsky, D. G.; Verma, D.; Prier, C. K.; Scholes, G. D.; Hyster, T. K. Using Enzymes to Tame Nitrogen-Centred Radicals for Enantioselective Hydroamination. *Nat. Chem.* **2023**, *15* (2), 206−212.
(28) Zhang, Z.; Feng, J.; Yang, C.; Cui, H.; Harrison, W.; Zhong, D.; Wang, B.; Zhao, H. Photoenzymatic Enantioselective Intermolecular Radical Hydroamination. *Nat. Catal* **2023**, *6* (8), 687−694.
(29) Ouyang, Y.; Turek-Herman, J.; Qiao, T.; Hyster, T. K. Asymmetric Carbohydroxylation of Alkenes Using Photoenzymatic Catalysis. *J. Am. Chem. Soc.* **2023**, *145* (31), 17018−17022.
(30) Chen, X.; Zheng, D.; Jiang, L.; Wang, Z.; Duan, X.; Cui, D.; Liu, S.; Zhang, Y.; Yu, X.; Ge, J.; Xu, J. Photoenzymatic Hydrosulfonylation for the Stereoselective Synthesis of Chiral Sulfones. *Angew. Chem., Int. Ed.* **2023**, *62* (23), No. e202218140.
(31) Toogood, H. S.; Scrutton, N. S. Discovery, Characterization, Engineering, and Applications of Ene-Reductases for Industrial Biocatalysis. *ACS Catal.* **2018**, *8* (4), 3532−3549.
(32) Fu, H.; Cao, J.; Qiao, T.; Qi, Y.; Charnock, S. J.; Garfinkle, S.; Hyster, T. K. An Asymmetric Sp3−Sp3 Cross-Electrophile Coupling Using 'Ene'-Reductases. *Nature* **2022**, *610* (7931), 302−307.
(33) Page, C. G.; Cao, J.; Oblinsky, D. G.; MacMillan, S. N.; Dahagam, S.; Lloyd, R. M.; Charnock, S. J.; Scholes, G. D.; Hyster, T. K. Regioselective Radical Alkylation of Arenes Using Evolved Photoenzymes. *J. Am. Chem. Soc.* **2023**, *145*, 11866.
(34) Sandoval, B. A.; Clayman, P. D.; Oblinsky, D. G.; Oh, S.; Nakano, Y.; Bird, M.; Scholes, G. D.; Hyster, T. K. Photoenzymatic Reductions Enabled by Direct Excitation of Flavin-Dependent "Ene"-Reductases. *J. Am. Chem. Soc.* **2021**, *143* (4), 1735−1739.
(35) Tanner, D. D.; Singh, H. K. Reduction of Alpha-Halo Ketones by Organotin Hydrides. An Electron-Transfer-Hydrogen Atom Abstraction Mechanism. *J. Org. Chem.* **1986**, *51* (26), 5182−5186.
(36) Ghisla, S.; Massey, V.; Lhoste, J.-M.; Mayhew, S. G. Fluorescence and Optical Characteristics of Reduced Flavines and Flavoproteins. *Biochemistry* **1974**, *13* (3), 589−597.

https://doi.org/10.1021/acscatal.3c03771
ACS Catal. 2023, 13, 14680−14684